Review

Strategies and Challenge of Thick Electrodes for Energy Storage: A Review

Junsheng Zheng [1,*], Guangguang Xing [1], Liming Jin [1,*], Yanyan Lu [1], Nan Qin [1], Shansong Gao [3] and Jim P. Zheng [2]

[1] Clean Energy Automotive Engineering Center and School of Automotive Studies, Tongji University, Shanghai 201804, China
[2] Department of Electrical Engineering, University at Buffalo, The State University of New York, Buffalo, NY 14260, USA
[3] China Shenhua Coal to Liquid and Chemical Shanghai Research Institute, Shanghai 201108, China
* Correspondence: jszheng@tongji.edu.cn (Junsheng Zheng); limingjin@tongji.edu.cn (Liming Jin).

Abstract: In past years, lithium-ion batteries (LIBs) can be found in every aspect of life, and batteries, as energy storage systems (ESSs), need to offer electric vehicles (EVs) more competition to be accepted in markets for automobiles. Thick electrode design could reduce the use of non-active materials in batteries that its energy density would be improved and its cost would be cut. However, thick electrodes are limited by their weak mechanical stability and poor electrochemical performance, these limitations could be classified as the critical cracking thickness (CCT) and the limited penetration depth (LPD). The understanding of the CCT and the LPD have been proposed and the recent works on breaking the CCT and improving the LPD are listed in this article. By comprising these attempts, some thick electrodes could not offer higher mass loading or higher accessible areal capacity that would defeat the purpose.

Keywords: thick electrodes; critical cracking thickness; limited penetration depth; mass loading; area capacity

1. Introduction

Over the past few decades, lithium-ion batteries (LIBs) have attracted more attention as energy storage systems (ESSs) due to the strive for a greener future. A LIB is an electrochemical ESS that supply energy by electrochemical reactions occurred in porous electrodes. The introduction of LIBs into vehicles has required more demands for advanced batteries, a typical areal capacity for hybrid electrical vehicles (HEVs) is about 2 $mAh \cdot cm^{-2}$ while for typical electrical vehicles (EVs) is 4 $mAh \cdot cm^{-2}$ for state-of-the-art LIBs[1]. Energy to weight ratio is a critical issue for ESSs, and a battery level specific energy of ~225 $Wh \cdot kg^{-1}$ is widely accepted that combines the weight and driving mileage for EVs[2]. To offer advantages for EVs in market compete, the US Department of Energy (US DOE) and the Advanced Battery Consortium (USABC) held that the EVs should provide a range of at least 500 km while batteries as ESSs need to possess high energy density of approximately 235 $Wh \cdot kg^{-1}$ and 500 $Wh \cdot L^{-1}$ at battery pack level[3, 4].

For a greener future, China Society of Automotive Engineers (CSAE) with the guidance from Ministry of Industry and Information Technology of China (China IIT) publishes Technology Roadmap of Clean and New Energy Vehicles 2.0 that set a higher demand of 500 $Wh \cdot kg^{-1}$ on advanced batteries for EVs in 2035[5]. The US DOE organized a *Battery 500 Consortium* that aims to achieve battery energy above 500 $Wh \cdot kg^{-1}$, and some feasible strategies (see Fig. 1a) are given for lithium metal batteries. In general, advanced strategies proposed to obtain high energy storage systems include: (1) to study the new electrochemical energy storage mechanism[6]; (2) to broaden the cell potential window[7]; (3) to develop electrode materials with high specific capacity[8]; and (4) to design electrodes with high mass loading[9]. There are much studies that focus on developing next-generation high-energy batteries, such as Li-oxygen and Li-sulfur batteries. A high energy

Preprints (www.preprints.org) | NOT PEER-REVIEWED | Posted: 23 December 2022 doi:10.20944/preprints202212.0437.v1

density lithium-oxygen battery based on a reversible four-electron conversion to lithium oxide was reported[6]. However, most studies so far have focused on energy density on materials level while the specific energy density of the represent battery packs is nearly four times smaller than the energy density on material level (Fig.1b)[10]. Much non-active but indispensable components are introduced into batteries due to the need for its operation and management. Therefore, the improvement on material or electrode level could not completely transfer to battery level. To cut the gap on specific energy density between material level and battery level brings a brighter prospect to improve battery energy density and the fourth path is based on this idea. Furthermore, the first three ways make efforts on material or electrode level and need to put much energy on new mechanisms while the fourth path not. And the fourth path could further to improve energy density on battery pack level based on the first three ways.

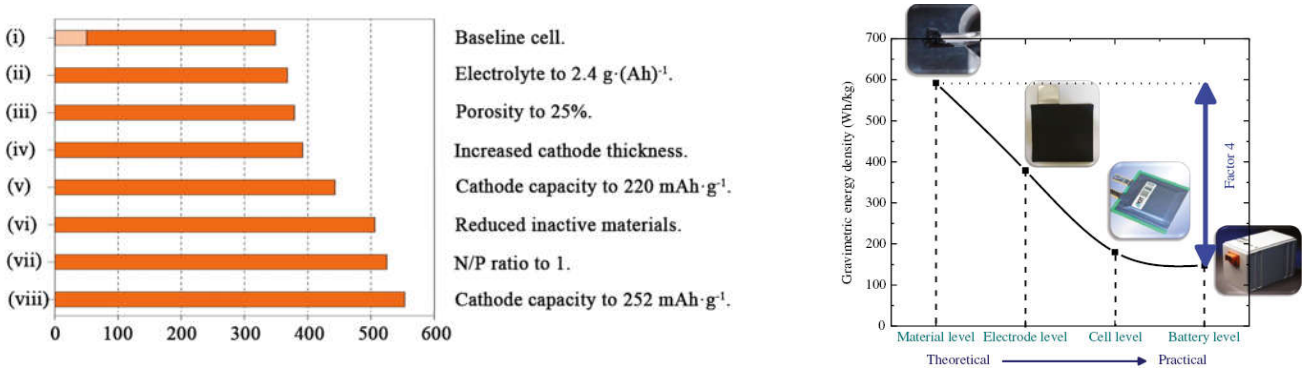

(**a**) (**b**)

Figure 1. (a) Calculated cell-level specific energy based on different strategies[11]. (b) The specific energy density based on a standard 52Ah pouch cell and state-of-the-art packs[10].

The fourth path that to design electrodes with high mass loading is thick electrodes. The principle of thick electrode design is that higher mass loading could decrease the share of non-active materials like current collectors and separators. However, it does not mean that the thicker the electrodes thickness the higher battery energy density. Fig. 2a gives the advantage of thick electrodes, and the trend of curves supports that point. For further vividly explain this principle, taking the commercial laminated batteries for example (see Fig. 2b), a repeating unit that contains electrode materials and current collectors and separators could be extracted. When using thick electrodes replaces the conventional electrodes in the repeating unit, the ratio of non-active materials in batteries is significantly decreased. The strategy of thick electrodes is to minimize the use of non-active materials to improve the battery energy density. And from Fig. 2b the use of non-active materials in batteries constructed by thick electrodes is already too low which means that there is not more space for improving battery energy density from increasing electrode thickness. It is agreed with the second half curves in Fig. 2a. Therefore, there exists an optimal interval of thickness or mass loading for electrodes, as shown in Fig. 2c. However, the concrete values are related various factors and not given.

In presently commercial LIBs, the thickness of electroactive components including the cathode and the anode are both limited between 50 and 100 μm[12, 13]. The design of thick electrodes is not a novel strategy and its application restricted by two serious obstacles that weak mechanical stability in production and poor electrochemical performance in working. It has been acknowledged in academe that there are two critical thickness for battery electrodes with high mass loading, one is the critical cracking thickness (CCT) about mechanical stability[14-17], the other is the limited penetration depth (LPD) for electrolyte transport in the electrode[2, 18-20].

In past years, much of studies were devoted to newly electrode design with high mass loading to boost the development of LIBs. For breaking the limitation of CCT, the

Preprints (www.preprints.org) | NOT PEER-REVIEWED | Posted: 23 December 2022 doi:10.20944/preprints202212.0437.v1

plentiful works draw the support of three-dimensional frameworks to offer mechanical stability[9, 21-25]. Electrodes with a thickness up to 850 μm and an aerial mass of 55 mg·cm^{-2} have been constructed with the aid of wood template[26]. For improving the limitation of LPD, to construct the ordered pores to decrease tortuosity is the most choices[27-29]. Thickness-independent electrodes constructed by vertical alignment of two-dimensional flakes could enable directional ions transport[30].

It is noteworthy that the limitations of ion diffusion in the liquid electrolyte deteriorate the rate capabilities of thick electrode design[2, 31]. Therefore, introducing thick electrode design into all-solid-state lithium batteries (ASSLBs) could be helpful due to the uniform transference number of inorganic solid electrolytes[32]. Moreover, the current ASSLBs are produced by expensive and multi-step processes based on thin-layer-deposition techniques and much efforts have been invested in increasing electrode thickness[33]. The combination of the two concepts could offer higher energy density and power density for lithium batteries. Hong et al. developed a new solvent-free dry technique to produce thick electrodes for ASSLBs which uses a Li^+-conducting ionomer as a binder to form fibrous linear binding[34].

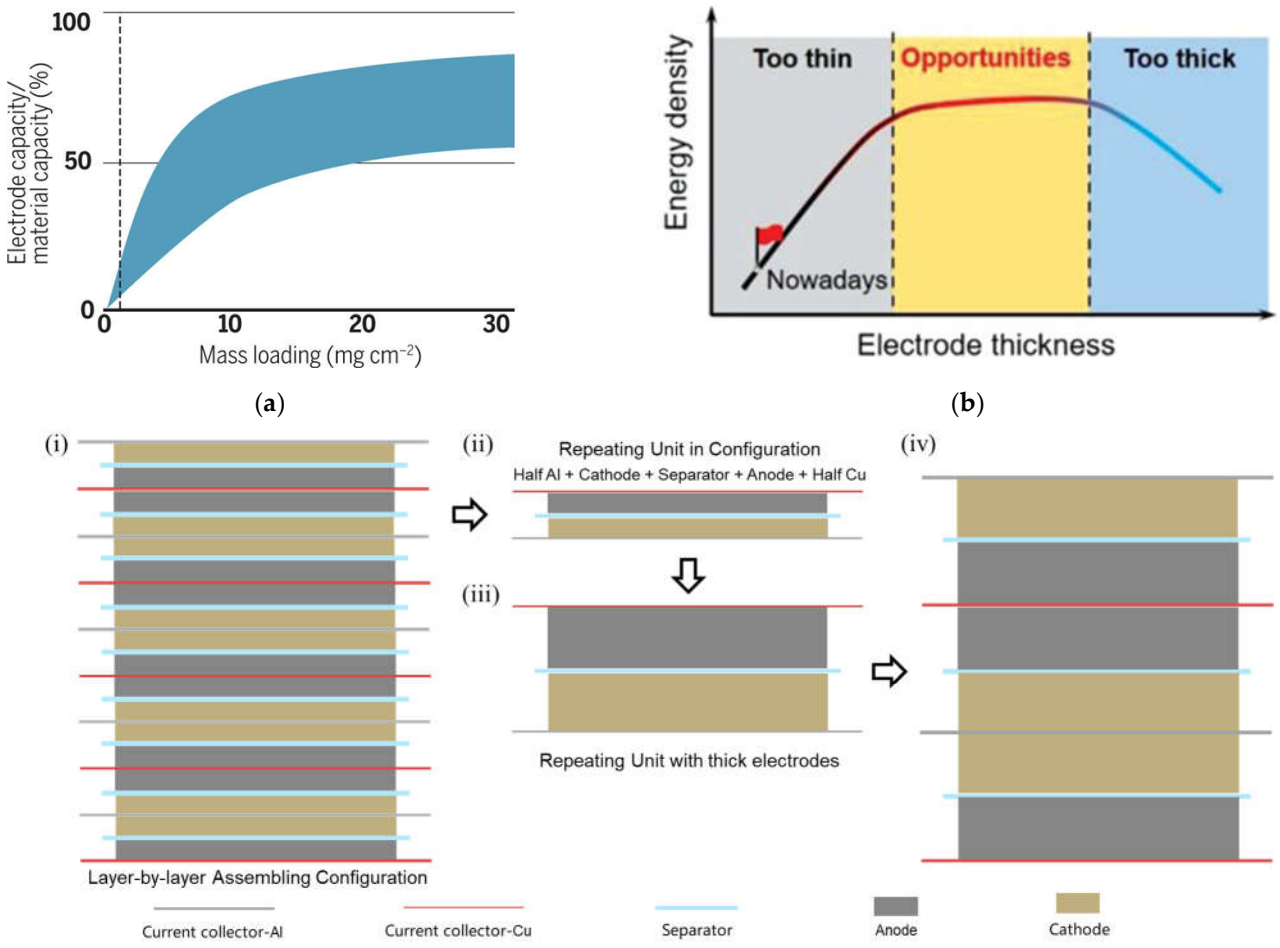

Figure 2. (a) The capacity of an electrode is positively proportional to the mass loading of active materials on the electrode[35]. (b) A detailed explanation about thick electrode design. (c) The opportunities for thick electrode design[36].

Here, recent progress in thick porous electrodes will be described and discussed for each point of view, including the understanding of the two critical thicknesses, the breakthrough in the two critical thicknesses, as well as the relevant comparison between these studies.

Preprints (www.preprints.org) | NOT PEER-REVIEWED | Posted: 23 December 2022 doi:10.20944/preprints202212.0437.v1

2. The challenge of thick electrodes

To obtain high energy density of 500 Wh·kg^{-1} for advanced batteries is the shared goal for China and US governments where are the largest automotives markets in the world. The *Battery 500 Consortium* proposed pathways to 500 Wh·kg^{-1} practical cells and an essential requirement is increasing the cathode thickness[11]. LIBs constructed by thick electrodes with high mass loading can benefit both vehicular range and unit cost in the application for EVs[37, 38]. The superiority of thick electrode design has been discovered formerly and the electrode thickness has been increased to over 100 μm in commercial batteries. Therefore, there must be some problems hindering the realization of thicker electrodes.

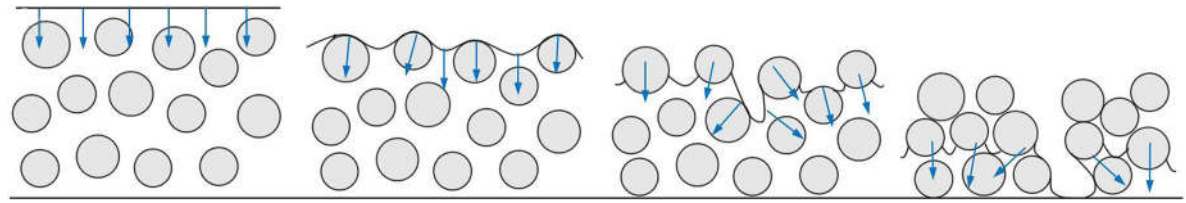

(a)

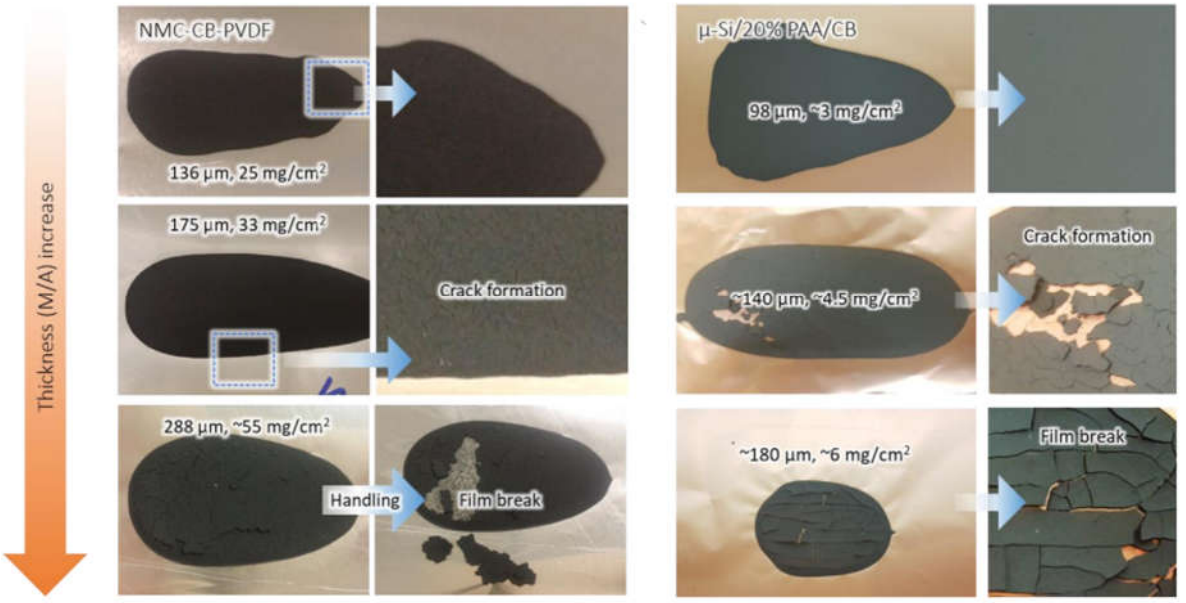

(b)

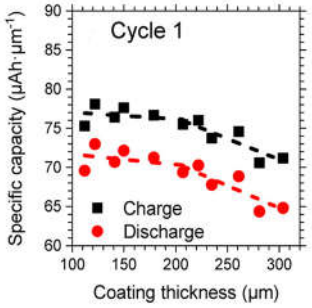

(c)

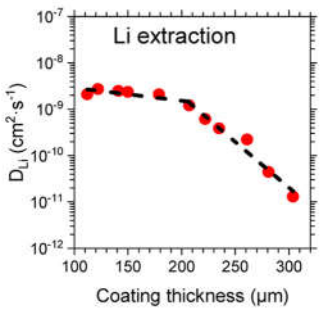

(d)

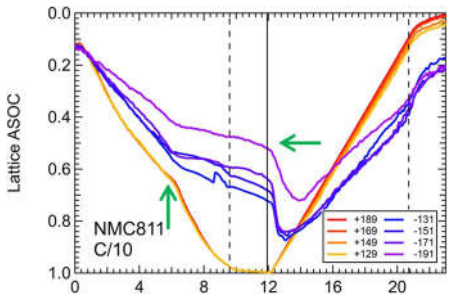

(e)

Figure 3. (a) Illustration of the drying process[39]. (b) Cracks in NMC electrodes (NMC811: PVDF: CB=90:5:5, wt.%) and μ-Si electrodes (μ-Si: PAA: CB=80:10:10, wt. %)[40]. (c) First cycle thickness-normalized specific capacity as a function of electrode thickness[41]. (d) D_{Li^+} as a function of electrode thickness[41]. (e) An inhomogeneity in different thicknesses across an NMC811 electrode during the charging and discharging process[42].

Preprints (www.preprints.org) | NOT PEER-REVIEWED | Posted: 23 December 2022 doi:10.20944/preprints202212.0437.v1

2.1. The critical cracking thickness (CCT)

During the drying of wet films, cracks were observed in diverse systems such as desiccated soil, concrete casting, ceramics slips, and model colloidal dispersions[43, 44]. Fig. 3a give the diagram about the drying process[39]. It has been widely accepted that the capillary stresses during drying process are the cause of cracking formation[14, 45-47]. When the slurry containing suspended particles is dried, capillary stresses are generated between particles in the air-solvent interface. If the particles are soft, they can remove stresses. But in reverse case, the stresses are released by cracks formation when the particles are hard[14].

It has been observed that the CCT would increase with the increase of particle size and be not affected by the drying speed[14, 17, 39]. It is noteworthy that lower drying speed has positive effects on the fracture toughness but not the film thickness[46]. It has also proven that drying rate actually has not an impact on the CCT but crack size[48]. And decreasing film thickness and increasing particle shear modulus would increase the critical capillary pressure for cracking formation. Singh et al. analyzed the influencing factors of the capillary stresses and established a formula about the CCT:

$$h_{max} = 0.41\left(\frac{GM\emptyset_{rcp}R^3}{2\gamma}\right)^{1/2}, \quad (1)$$

where h_{max} is the CCT, G is the shear modulus of the particles, M is the coordination number, $\emptyset_{rcp}$ is the particle volume fraction at random close packing, R is the particle radius, and γ is the air-solvent interfacial tension[14].

The traditional and mature technology in electrode manufacture is to mix active materials with conductive additives and binders in organic solvents, and then to coat this slurry on current collectors like Al or Cu film. And a requisite step in this manufacture is to evaporate the solvents. The cracks also have been observed on battery electrodes, cracks were generated in NMC electrodes (NMC811: PVDF: CB=90:5:5, wt.%) at a thickness above 175 μm and any crack-free μ-Si electrodes (μ-Si: PAA: CB=80:10:10, wt. %) could not be fabricated at a thickness above 100 μm, as depicted in Fig. 3b[40].

2.2. The limited penetration depth (LPD)

High mass loading electrodes would increase the thickness of electrode films, which increases the diffusion distance of charges in electrodes. The longer diffusion distance of charges reduces the mass transport efficiency during the electrochemical process[19]. And due to the sluggish ions transport kinetics, not all active materials in thick electrodes could be used in high C-rates. It has been proven that the limited diffusion of Li^+ inside the porous electrode leads to the under-utilization of the active material[12, 41, 49, 50].

When the LPD is greater than the designed electrode thickness, mass transport in electrolyte would not be the limited factors of the full utilization of active materials in electrodes[2]. To balance the migration of anions that do not participate in the electrochemical process a lithium salt concentration gradient would form that is what the LPD means[18]. The LPD is in inverse proportion to C-rates and tortuosity[20]. And a simple analytical equation for the LPD for electrolyte transport in the electrode is given:

$$L_d = \frac{\varepsilon}{T}\frac{D_0 c_0 F}{(1-t_+)I}, \quad (2)$$

where L_d is the LPD, ε is the porosity of the electrode, T is the tortuosity factor of the pore matrix, D_0 is the diffusion coefficient of the lithium salt species in the electrolyte, c_0 is the initial concentration of electrolyte, t_+ is the transference number of Li^+, I is the applied current density and F is the Faraday constant[2].

From experiments on NMC622 electrodes with different thicknesses, their specific capacities at C/50 rate were obtained and these values were normalized by their coating thickness[41]. An obvious turn at ~200 μm was shown in the plot of the normalized capacity as the function of thickness, as shown in Fig. 3c. Moreover, the lithium diffusion coefficient (D_{Li^+}) that calculated from GITT is a related parameter of Li+ diffusion behavior.

 doi:10.20944/preprints202212.0437.v1

The same turn at ~200 μm were observed in the plot of D_{Li^+} as the function of thickness (see Fig. 3d). And the operando studies about the depth-dependent inhomogeneity are support this suspect, as shown in Fig. 3e[42]. The same result has been proposed that the maximum film thickness limited by ions diffusion is approximately 200 μm[30].

The ESSs for EVs are required in excellent performance in terms of energy and power. To fabricate battery electrodes with high mass loading needs to break the limit of the CCT, and the LPD is the obstacle that stand in the way of battery electrodes with high accessible areal capacity. According to the understanding of the CCT and the LPD, various ways have been developed to solve the problems.

3. Strategies for increasing electrode thickness

Making thick electrodes a reality needs to break the limitations of CCT and LPD. And how to fabricate crack-free electrodes is the first concern, which means the solution could be two-steps or one-step. The two-steps solution is to solve those two problems separately, for example, a thick and free-standing electrode was constructed with two-dimensional nanomaterials that breaks the CCT and then a laser drilling technique was adopted to fabricate a micro-hole array in this electrode to increase the LPD[51]. The one-step solution is to solve those two problems simultaneously, for example, an ultra-thick electrode fabricated by wood-template which template as frameworks could improve mechanical stability and the gaps formatted during drying process between active materials and carbon frameworks could improve diffusion kinetics[52].

3.1. Increasing the CCT

From the formation mechanism, the cause of cracking is generated stresses during drying process[14, 17, 39], and even is the traditional technology (the wet-slurry casting technology) from a higher vision. Therefore, there are three strategies to construct thicker electrode. One is making efforts to decrease the generated stresses during drying process, another is using three-dimensional (3D) frameworks to offer mechanical stability while the other is taking new manufacture technologies beyond the traditional technology.

3.1.1. Decreasing generated stresses

According to h_{max} ~ $(1/\gamma)^{1/2}$ from Eq. 1, the CCT could be improved by decreasing the surface tension. Thus, making efforts to decrease the surface tension is a straightforward method to alleviate or eliminate cracks. According to this point, Du et al. have successfully constructed a NMC532 electrode with areal loading above 25 mg·cm^{-2} (~ 4 mAh·cm^{-2}) by introducing isopropyl alcohol (IPA) into aqueous solvent systems to decrease the surface tension, as shown in Fig. 4a[39].

As shown in Fig. 4b, the remaining particles are forced to fill a certain ratio of the formed void when the solvent is evaporating during drying process. And cracking would occur when above a certain value. Therefore, the other way to reduce mechanical stresses is to reduce the amount of solvent which needs to be inevitably evaporated during drying process[47]. By increasing the solid content of the electrode slurry with using new binder system to 65 wt.%, crack-free NMC111 electrodes have been constructed with an active mass loading of up to 60 mg·cm^{-2} and an average dry film thickness of (322±9) μm[47].

Moreover, the observed results of NMC electrodes with different particle sizes are contrary to the estimate of h_{max}~R$^{3/2}$[53]. There is no contradiction, since the stresses are removed by particles itself when particles are soft or by cracks when particles are hard. And there are more than one kind particles in the electrode slurry. The NMC particles are hard, so the stresses are released by softer binders and conductive additives and even cracks. And a simple ball and spring model was given in Fig. 4c, to reduce the size of active particles would decrease stresses in binders and conductive additives. Therefore, the formation of cracks was reformed when NMC811 particles of smaller size were used.

Preprints (www.preprints.org) | NOT PEER-REVIEWED | Posted: 23 December 2022 doi:10.20944/preprints202212.0437.v1

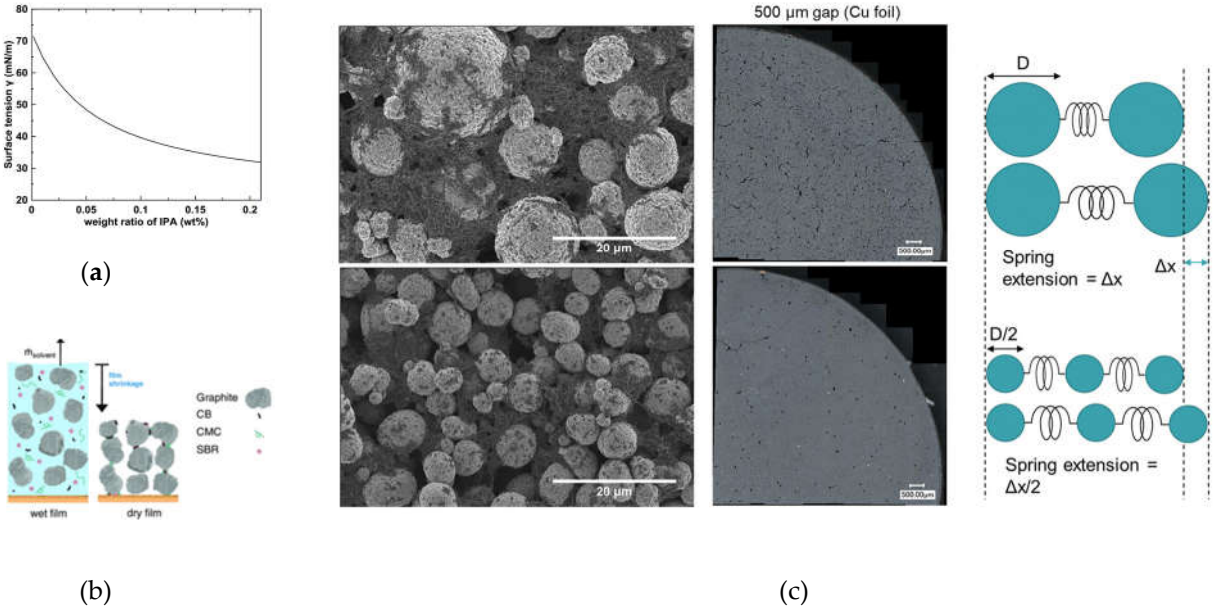

Figure 4. (a) Calculated surface tension of IPA-water mixture versus composition[39]. (b) Schematic of the wet film and dry film[48]. (c) SEM and optical microscope images of aqueous-processed cathode coatings (500 μm coating wet gap) on copper foil. And a simple ball and spring model is given[53].

3.1.2. Utilizing 3D frameworks

The mechanical stability of thick electrodes could draw support from 3D frameworks. Several thick and ultra-thick electrodes have been successfully fabricated with the aid of carbon frameworks[9, 21-23, 25], metal foams[13, 54-56], and 3D conductive textile[57]. Besides, some 3D frameworks could offer convenient ion and electron channels to improve the limited diffusion kinetics due to the increased thickness.

Carbon nanotubes (CNT) and carbon nanofibers (CNF) are easy to form crosslinked networks and provide features as both binders and conductive additives. Park et al. constructed a high-performance electrode with the thickness of up to 800 μm through segregated CNT networks, as shown in Fig. 5a[40]. Due to the improved mechanical robustness through these networks the extremely thick electrodes could be constructed. With the help of graphite fibers (GF) bonded with pyrolytic carbon (PC) and graphite nanoplatelets (GNP), an ultra-thick electrode with the thickness of 17 mm performed the reversible capacity of 11.63 mAh·cm^{-2} (as shown in Fig. 5b)[22]. And some carbon networks could undertake the functions of binders and conductive additives. It may be profitable for decreasing the ratio of non-active materials in battery electrodes.

Thicker electrodes could be constructed with the aid of 3D current collectors that all particles are not more than 50 μm from the nearest current collector. Metal foams have attracted more attention since they are the most suitable to introduce into the slurry casting process to fabricate electrodes. A graphite electrode was constructed with the thicknesses of 0.6 and 1.2 mm by using Cu foams as the current collector[13]. And Yang et al. fabricated a 450 μm thick graphene electrode with mass loading of 10~15 mg·cm^{-2} by using Al foams[55]. The 3D current collector also could improve kinetics of electrodes. From the comparison of foam-collector-type and foil-collector-type electrodes with similar mass loading of active materials, the charge transfer resistance was 7 times less for the foam than for the foil, at values of 15 and 110 Ω (as shown in Fig. 5c)[54], respectively. Furthermore, by comparing the cyclic voltametric curves for the cells using different sizes of metal foams, as shown in Fig. 5d, a remarkable result was that the peak became lower and wider for the cell using 1200 μm size of metal foams[56]. It indicated that using 3D current collector to fabricate electrodes could settle mechanical but not completely electrochemical problems in thicker electrodes.

Preprints (www.preprints.org) | NOT PEER-REVIEWED | Posted: 23 December 2022 doi:10.20944/preprints202212.0437.v1

Other 3D frameworks are also used to fabricated thick electrodes. The 3D conductive textiles have been introduced batteries electrodes due to its stable potential range in organic electrolyte and electrodes have been fabricated with a thickness of ~600 μm through 3D conductive textiles, which are 8-12 times higher of those on metal collector[57].

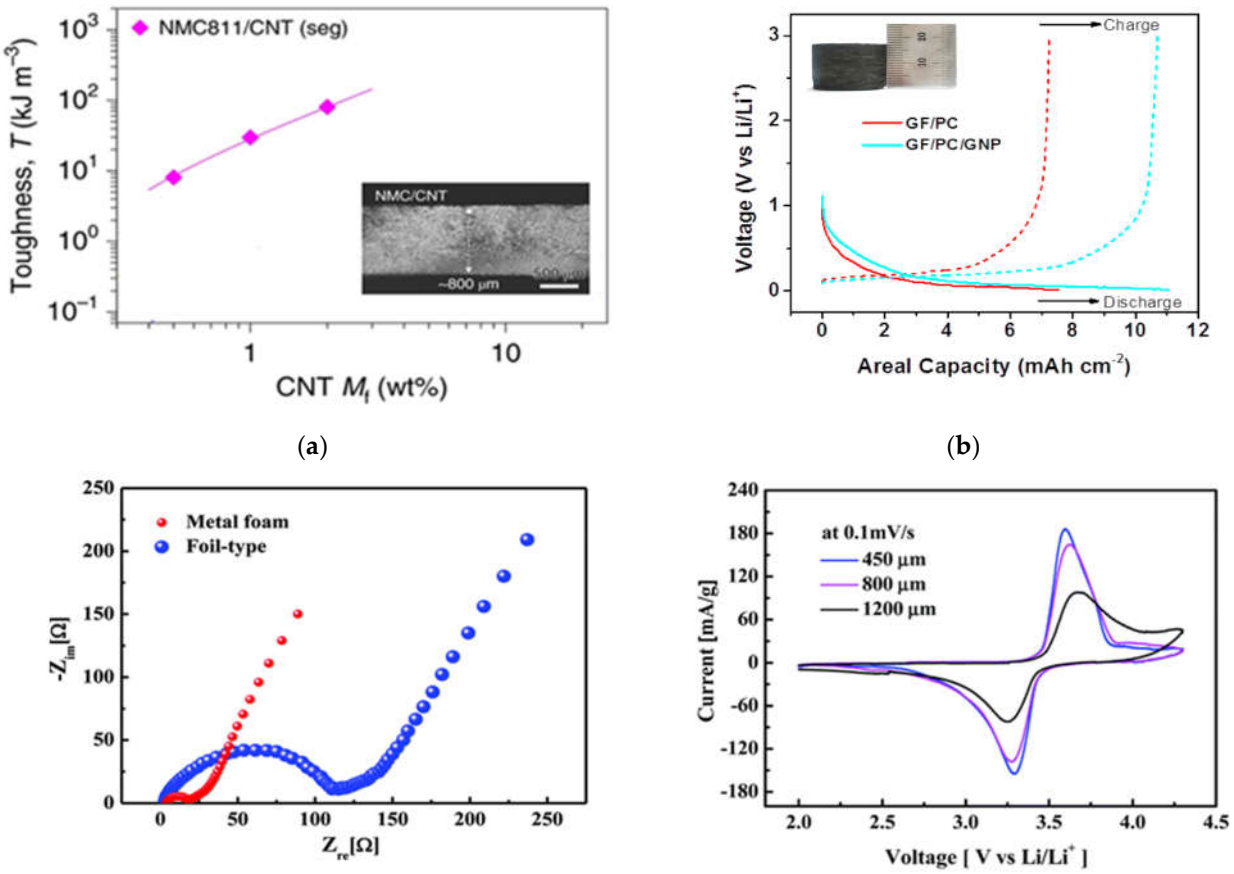

Figure 5. (a) Tensile toughness of NMC811/CNT electrodes plotted versus CNT content[40]. (b) The reversible capacity of the 3D thick all-carbon frameworks[22]. (c) Comparison of the impedance curves for electrodes constructed by the metal foam and the foil[54]. (d) Comparison of the cyclic voltametric curves for the electrodes using different cell size of metal foams[56].

3.1.3. Taking new technology

Since the cracks occur during drying process, taking some manufacture technologies without evaporation process are possible ways to construct crack-free thick electrodes. Some technologies have been successfully introduced into battery electrodes like spraying[58-60], sintering[61], 3D printing[62-65], powder extrusion moulding (PEM)[66-68] and dry powder coating[69, 70]. Solvent-free process is an ideal alternative solution to replace the wet slurry casting process. The related stresses generated during drying process would no longer consider. Moreover, manufacture costs would be cut as the elimination of using and removing solvents.

Preprints (www.preprints.org) | NOT PEER-REVIEWED | Posted: 23 December 2022 doi:10.20944/preprints202212.0437.v1

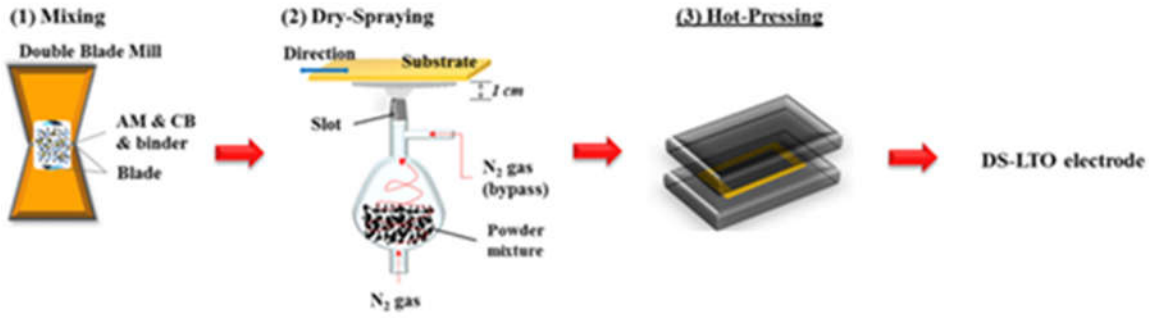

(a)

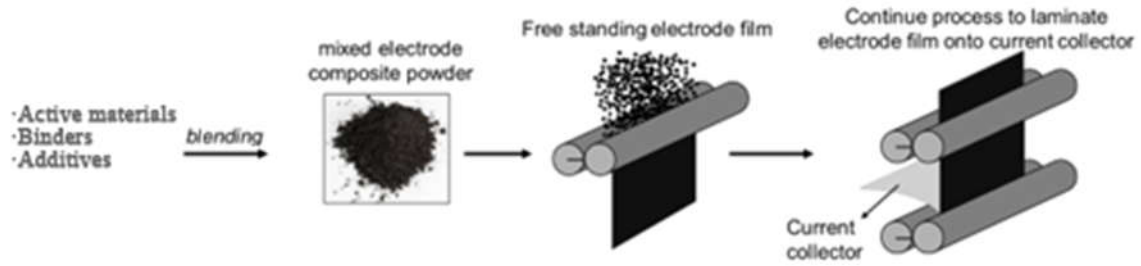

(b)

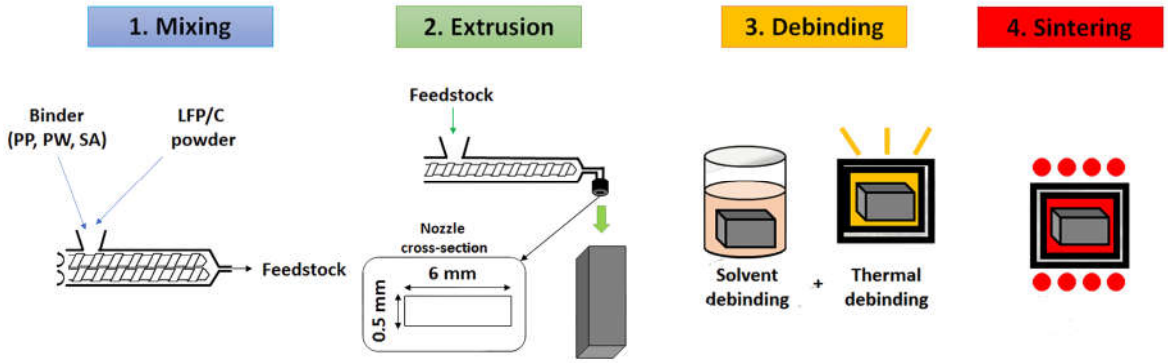

(c)

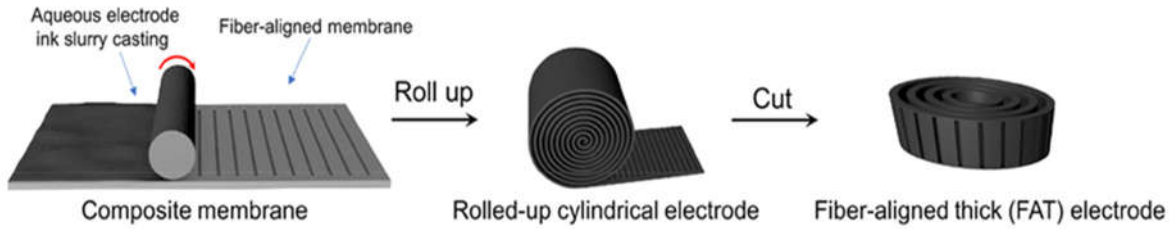

(d)

Figure 6. (a) A schematic of the dry spraying process[59]. (b) A schematic of the dry coating process. (c) Schematic illustrations of powder extrusion moulding[67]. (d) Schematic fabrication of fiber-aligned thick electrode[9].

A solvent-free technology is spray deposition that has been used in coating industries for over 30 years to create functional paints. Recently this technology has been introduced into producing battery electrodes. The main processes of this technology are mixing, dry-spraying and hot-pressing. Fig. 6a gives the optimized technology for using in battery electrodes and the fabricated LTO electrode has interconnected particles that facilitated electron and ion transport via shorten pathways within the electrodes[59]. And the film thickness could be controlled just by adjusting the spraying time[58].

Preprints (www.preprints.org) | NOT PEER-REVIEWED | Posted: 23 December 2022 doi:10.20944/preprints202212.0437.v1

Another solvent-free technology is dry coating technology that does not introduce any solvents into the craft, as shown in Fig. 6b. This technology maintains liquid-free state in the full process from the raw materials to finished products. Free-standing electrodes with thicknesses between 50 microns to about 1 millimeter could be easily fabricated by this craft. It has been proven that the bonding strength between dry-deposited particles and current collectors could be greater than slurry-cast electrodes[70].

PEM is also a cost-effective manufacturing method to produce battery electrode. Main steps of PEM are mixing, extrusion, debinding and sintering, as shown in Fig. 6c. Thick electrodes constructed by PEM technology shows better mechanical properties than alternative technologies[66]. The $Li_4Ti_5O_{12}$ (LTO) anodes and the $LiFePO_4$ (LFP) cathodes have been produced with the thickness as high as 500 μm through this method[66, 67]. And a LIB was assembled with this LTO anode and this LFP cathode and possessed mass loading of ~100 $mg \cdot cm^{-2}$ that is better than the current one[68]. Just as important, this technology is also an environmentally friendly technology for electrodes manufacturing.

Due to the low-cost and simple manufacturability Extrusion-based 3D printing is a potential craft for electrode fabrication. The thickness of thick electrodes could be well controlled thanks to the layer-by-layer additive technique[71]. Sun et al. constructed an ultra-thick LTO electrode by using 3D printing with the thickness of 1500 μm[62]. And 3D-printed electrodes with highly interconnected networks could offer ion- and electron-transport paths, which indicated a better electrochemical performance[63].

And a new design called fiber-aligned thick electrode has been used to construct thick electrodes. The composite membrane contained aligned carbon fibers could provide low tortuosity, high conductivity, and mechanically strong features for high mass loading electrodes and this novel design is shown in Fig. 6d[9, 72].

There are many attempts to improve mechanical stability for producing thick crack-free electrodes. In this part, we mainly focus on the growth of thickness. Some technologies also bring other gains, 3D current collectors could serve as both support and collector that improve constructions stability and electrons conductivity. The thick electrodes fabricated by 3D printing technology have advanced ions transport pathways due to the highly ordered structure. And solvent-free technologies no longer need the using and removing of solvents, as well the corresponding costs.

3.2. Increasing the LPD

Improving mechanical stability to fabricate crack-free electrodes is just the first step to get the target on energy density of 500 $Wh \cdot kg^{-1}$. When the porosity of thick electrodes is below 30%, it is found that ionic conduction within such a thick and dense electrode becomes a main reason that causes poor rate performances[2, 42, 73]. For thick electrodes, the ionic resistance in pores (R_{ion}) is higher than the charge-transfer resistance for Li intercalation (R_{ct}), as shown in Fig. 7a, so there are limited ions diffusion behaviors across thick electrodes[74].

According to Eq. 2 of the LPD, the LPD is proportional to the porosity of the electrode and inversely proportional to the tortuosity of the electrode. The diffusion coefficient of Li+ is the directly related to the diffusion behaviors of Li+ in porous electrodes. And a simplified expression could be inferred from Eq. 2:

$$D_{eff} = \frac{\varepsilon}{\tau} D_{Li} \tag{3}$$

where D_{eff} is the effective ionic conductivity, ε is the porosity of the electrode, τ is the tortuosity of the electrode and D_{Li} is the intrinsic ions conductivity[75-77].

Preprints (www.preprints.org) | NOT PEER-REVIEWED | Posted: 23 December 2022 doi:10.20944/preprints202212.0437.v1

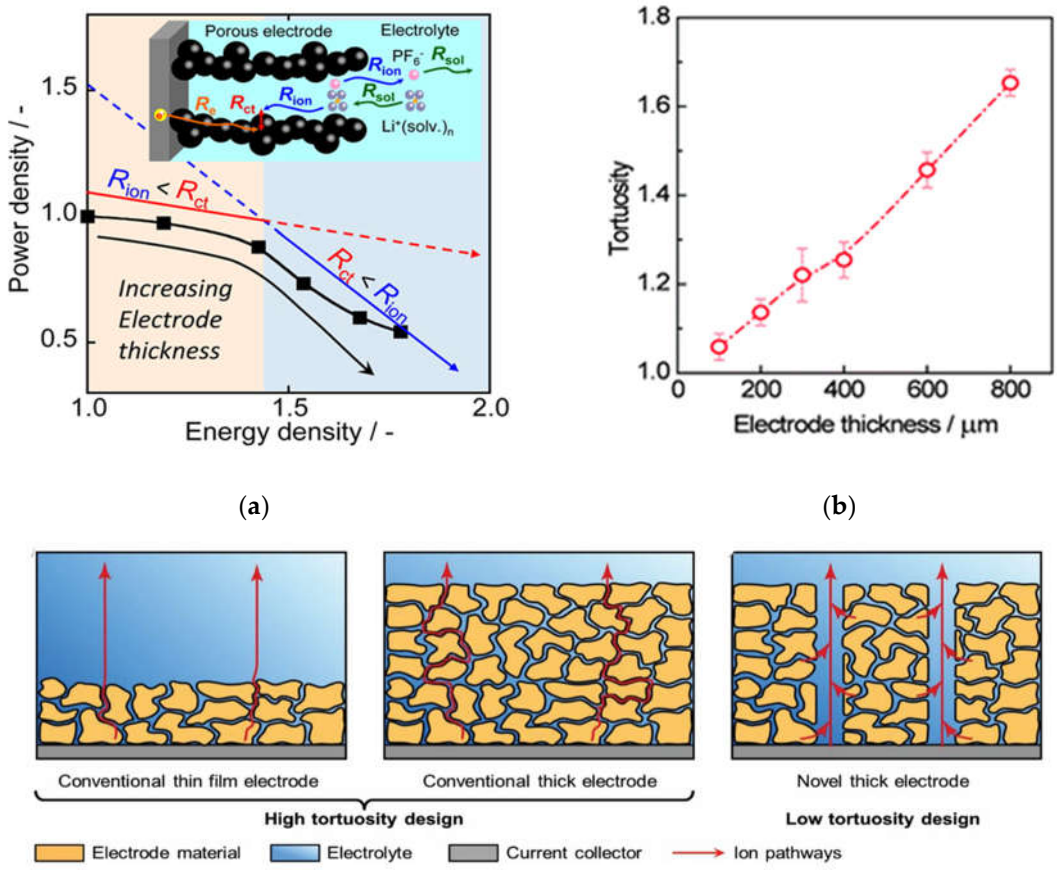

Figure 7. (a) The changes of R_{ion} and R_{ct} and their magnitude show opposite trends with respect to electrode thickness[74]. (b) Higher tortuosity is present in a thicker electrode[78]. (c) Illustration about the value of the low-tortuosity design for thick electrodes[36].

Therefore, there are two strategies to improve ions diffusion behaviors. One is to optimize porosity of the electrode to get better rate performance, the other is to construct vertically pathways to current collectors for fabricating low-tortuosity electrodes. However, a high porosity would reduce the ratio of active materials in electrodes and it goes against the design of thick electrodes. And Fig. 7b clearly shows that the tortuosity of the electrode increases with the growth of electrode thickness[78]. Therefore, the low-tortuosity design with building ions transport pathways paralleled to the direction of ions transmission has become a key principle for thick electrodes[27-29]. And the superiority of low-tortuosity design in thick electrodes could be obtained from Fig. 7c[36].

It is noteworthy that the low-tortuosity design would increase the porosity of the electrode in essence but this increase would bring more effective promotion on ions diffusion behavior. Moreover, there is an optimal design of the oriented porosity ε_0 and matrix porosity ε_m, which could balance the ion transport kinetics along the channels and in the matrix. And it has been given an optimal value ($\varepsilon_0 \approx 0.11$ at $\varepsilon_0+\varepsilon_m = 0.42$) at which the oriented-pore achieved the best rate capability without a sacrifice of the energy density[28].

3.2.1. Optimizing electrode porosity

When thick electrodes are discussed, not much attention has been paid to how dense the electrode is, since most of the testing end at coin cell level. However, the practical use of thick electrodes not only needs to consider their mass loading, porosity is equally important[79]. Fig. 8a revealed the role of the porosity that plays in the evolution of rate-limiting step in thick electrodes[49]. The porosity is critical for performing electrochemical

Preprints (www.preprints.org) | NOT PEER-REVIEWED | Posted: 23 December 2022 doi:10.20944/preprints202212.0437.v1

properties of electrodes. And some studies have proven that the electrochemical performance of thick electrodes could be improved through the porosity gradient[80, 81].

To put kinetics into perspective, the porosity across the electrode showing a gradient increase is beneficial from the region near to the current collector to the region close to the separator. The reason is that electrodes with large porosity near separators could facilitate fast ion transport while electrodes with small porosity close current collectors could ensure optimum electronic contact[80, 82-84]. Based on electrochemical porous-electrode model, two teams obtained the same results via distinct simulation methods that a gradient porosity where the porosity close to separators in electrodes is higher to accommodate more electrolyte could minimized the resistance across the electrode[80, 82]. Another report also supports this suspect, but it puts forward that it is not much use to construct graded electrode beyond 2 layers for reducing the resistance across the electrodes. Beyond simulations, the electrodes with staged porosity in order to improve ions migration has been constructed by applying the capillary suspension concept[84]. This strategy has under patent-pending protection application[85].

However, an opposite viewpoint has been given. The highest stresses located in the electrodes near the current collectors and increasing the porosity of this region the maximum stress could be reduced. Furthermore, the lower porosity of electrodes near separators would contribute to maintain a higher potential during discharge[81]. Moreover, the comparison of electrochemical performance between directional ice templating with low porosity nearest the separator (DIT LP-S) and directional ice templating with low porosity nearest the current collector (DIT LP-CC) shows that the former performed better rate capability (Fig. 8b-c)[86]. Similarly, this strategy also has patent protection[87].

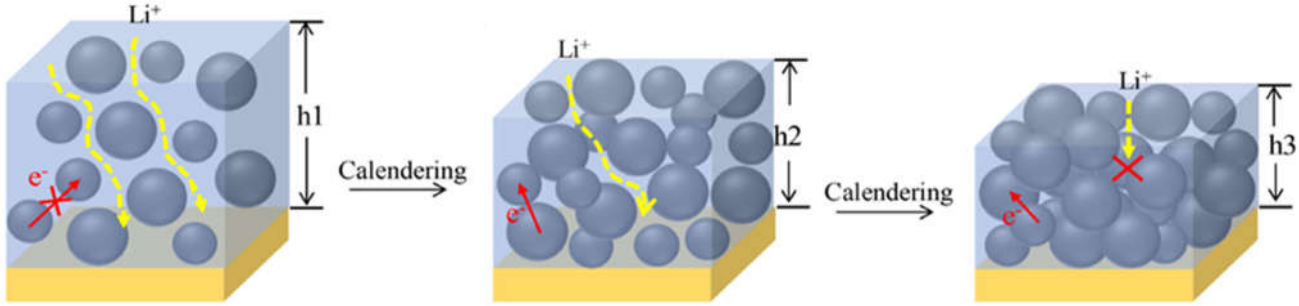

(a)

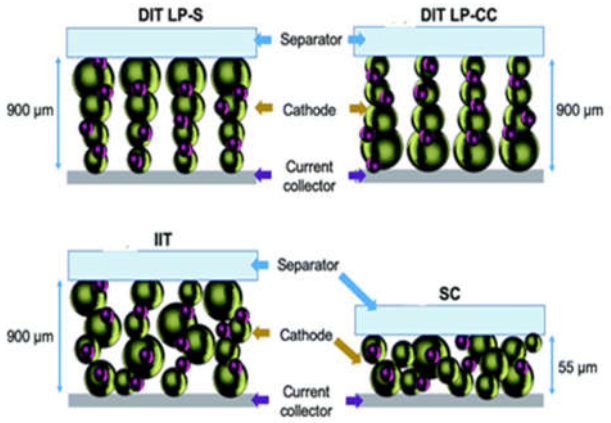

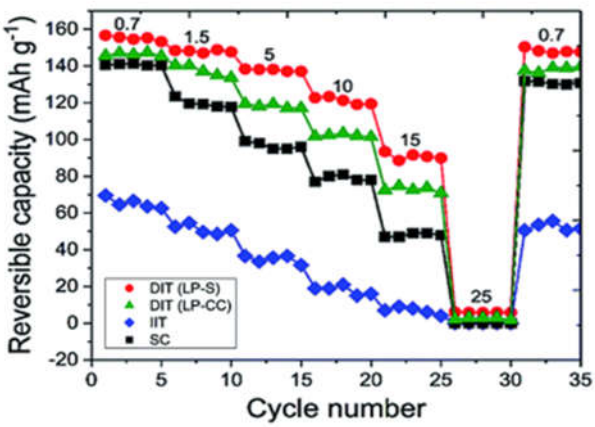

(b) (c)

Figure 8. (a) The charge transport in electrodes with different porosity[49]. (b) Schematics of the four electrode types fabricated for performance comparison: (i) directional ice templating with low porosity nearest the separator (DIT LP-S); (ii) directional ice templating with low porosity nearest

Preprints (www.preprints.org) | NOT PEER-REVIEWED | Posted: 23 December 2022 doi:10.20944/preprints202212.0437.v1

the current collector (DIT LP-CC); (iii) isotropic ice templating (IIT); and (iv) slurry casting (SC)[86]. (c) Reversible capacities of the four types of these electrodes at different current densities[86].

3.2.2. Decreasing electrode tortuosity

Fig. 8c also gives other sights that both DIT LP-S and DIT LP-CC electrodes performed better rate capability than isotropic ice templating (IIT) electrodes and the IIT electrodes also had poor rate performance than the traditional slurry casting (SC) electrode. Combining with Fig. 8b, these sights indicate that the increased thickness of electrodes would deteriorate the rate performance and decreasing electrode tortuosity could improve electrochemical performance in thick electrodes. Furthermore, more general and sustainable approaches are highly desired to fabricate uniformly aligned microchannels in the electrode.

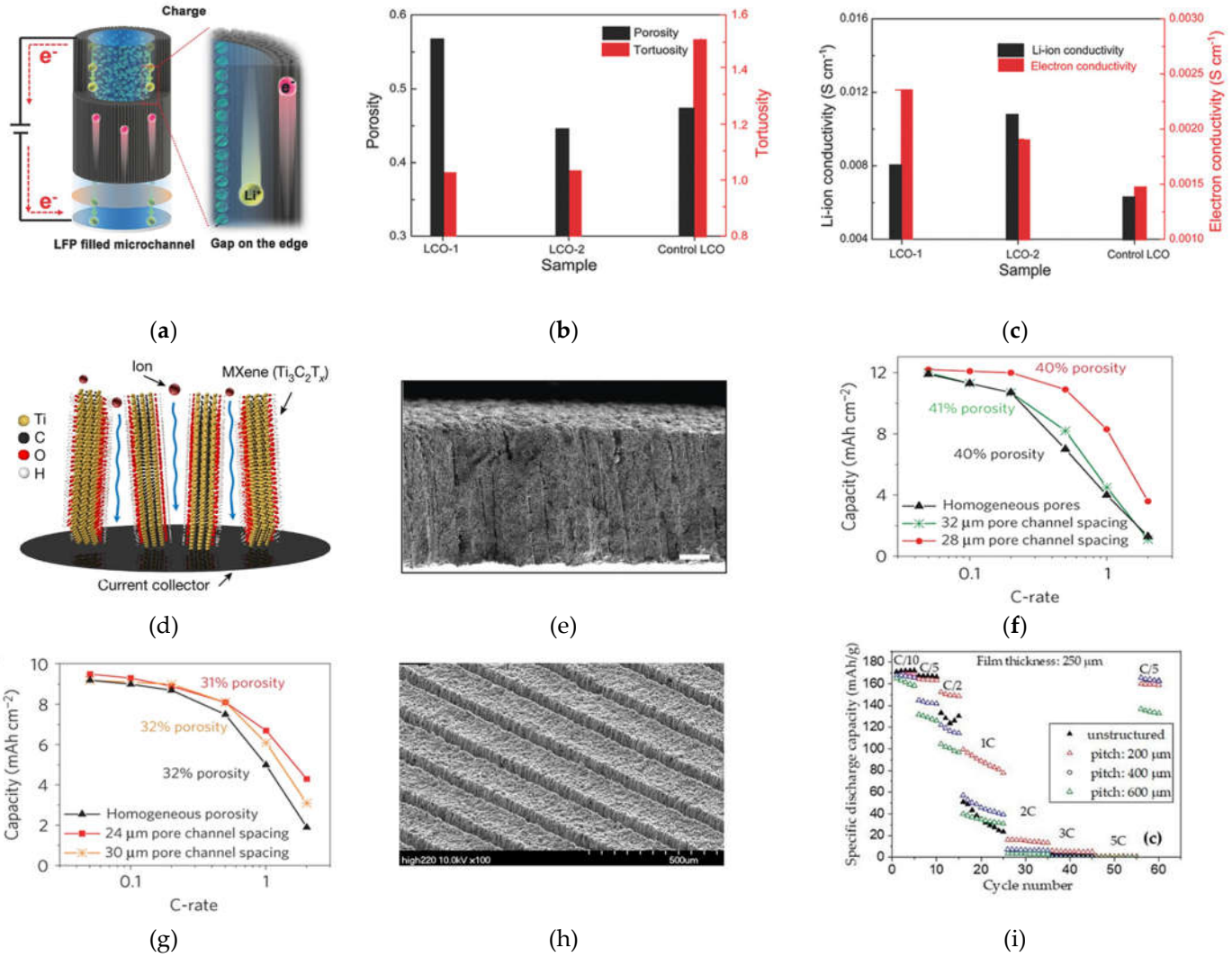

Figure 9. (a) Graphical illustrations of the ion and electron transportation behavior occurring in the wood-templated electrodes[52]. The comparison of LCO-1, LCO-2, and control LCO in terms of (b) tortuosity and porosity, (c) Li-ion and electron conductivities[88]. (d) Schematic illustration of ion transport in vertically aligned $Ti_3C_2T_x$ MXene films[30]. (e) Cross-sectional SEM image of a low tortuosity LCO electrode constructed by magnetic method[89]. Areal capacity versus C-rate for LCO electrodes with pore channels: (f) 310-μm-thick electrodes with 39-42% porosity and (g) 220-μm-thick electrodes with 30-32% porosity[90]. (h) SEM images for laser-structured electrodes (thickness≈210 μm)[91]. (i) Specific discharge capacity of cells containing 250 μm thick electrodes with different pitch distances[92].

 doi:10.20944/preprints202212.0437.v1

To build up hierarchical microstructures for improving the performance of electrodes, nature has provided us many templates and inspirations[93]. Along the growth direction wood has open channels for transferring water, ions and other ingredients, which offers a guide for fabricating electrodes with ordered structures. Thick electrodes constructed via wood template inherit directional porous structure where provides pathways for ease ions and electrons transport across the entire electrode[23, 26, 94-96]. As shown in Fig. 9a, the interconnected carbon framework could provide a conductive network for electrons transport while the gap between active materials and frameworks could offer low-tortuosity pathways for ions transport[52]. To further illustrate the value of wood-template, Lu and coworkers constructed the traditional LiCoO2 cathode (control LCO) and the wood-template LiCoO2 cathodes (LCO-1 and LCO-2, the LCO-2 for higher mass loading underwent the double processes of LCO-1) and measured their related properties[88]. The results are given in Fig. 9b-c, and the tortuosity of wood-template cathodes is approximately close to 1 due to ordered microchannels and smaller than the control LCO. The ion conductivity and electron conductivity of wood-template cathodes are larger than the control LCO. Through comparing the porosity and ion conductivity between LCO-1 and LCO-2, a larger porosity is not always positive to improve ions diffusion or the LPD.

Ice-template technique is also used to build orientational pores for ions migration[64, 86, 97]. The ordered pores could be well controlled by adjusting the freezing and sintering parameters. Electrodes fabricated by this technique could combine the energy and the power[97]. Moreover, Miller et al. successfully constructed thick electrodes with the thickness-independent electrochemical performance by aligning vertical two-dimensional flakes[72]. And Fig. 9d gives a scheme of thick electrodes constructed by this guidance, and approximately 200 μm is the maximum thickness of each film due to the ion transport limitations[30]. It is another proof of the LPD.

Commercial availability is also a critical factor for building directional aligned pores in electrodes. And a simple, up-scalable and inexpensive technique to construct pathways paralleled to the direction of the Li+ migration has been proposed by applying a magnetic field during the electrode fabrication (Fig. 9e)[89, 90, 98-101]. A magnetic control method based on sacrificial features was reported, magnetized nylon rods or magnetic emulsions were used as template to fabricate directional aligned pore arrays in the thick electrode[90]. And it is noteworthy that the aligned pore structure performs higher areal capacity under the same conditions (at constant thickness and total porosity) and smaller pore spacings are superior, as shown in Fig. 9f-g.

Moreover, Fig. 9f-g give a critical viewpoint that the pore parameters (like diameter, spacing) play a pivotal key on rate performance of electrodes. Therefore, a more precise technique for constructing vertical aligned pores is requested and essential. The laser-based manufacturing process attracts more attention in the low-tortuosity design for thick electrodes. This concept involves high-precision ablation of a small fraction of the active material from the initial coating and generating additional diffusion pathways (Fig. 9h)[10, 102]. The laser processing on electrodes is inevitably accompanied by slight capacity loss but significant improvements in rate performance[91, 103, 104]. By using 200 ns-laser radiation and a pitch distance of 200 μm, the loss in active material can reach values of about 30 wt.%, while a pitch distance of 600 μm would reduce the material loss below 10 wt.%[105]. And the rate performance in different pitch distances were given in Fig. 9i[92].

Furthermore, the ultrashort pulse duration in the femtosecond (fs) or picosecond (ps) range is less than the heat diffusion time, the ablation volume is emitted before any heat diffusion or thermal damage occurs and side effects are significantly reduced[106]. And due to the cold nature of fs-laser ablation, a high-aspect ratio of approximately 15 could be reached, which related to the capacity loss. So, the fine and accurate aligned pores array could be constructed. And the ideal pore parameters for maximizing the rate capability could be identified by evaluating the ions distribution in electrodes[107]. Furthermore,

Preprints (www.preprints.org) | NOT PEER-REVIEWED | Posted: 23 December 2022 doi:10.20944/preprints202212.0437.v1

the surface on laser-generated structures lead to an accelerated and homogenous wetting of the electrodes with liquid electrolyte[104, 105].

3.3. Summary

Table 2. Summary of recently reported thick electrodes.

Active materials	Thickness/ **μm**	Mass loading/ mg·cm^{-2}	Areal capacity/ mAh·cm^{-2} @ mA·cm^{-2}	Volumetric capacity/ mAh·cm^{-3}	Reference
LTO	~1500	30	4.74@1.06	31.6	[62]
LFP/C	240	12	1.86@1.02	77.5	[54]
NMC111	305	82	9.2@1.27	301.6	[108]
LMO	200	13	1.9@0.91	95	[109]
LTO	475	138	15.2@1.02	319	[66]
LCO	600	115.4	15.7@0.5	261.7	[32]
LFP	1000	36	5.5@1.22	55	[110]
LTO	1000	34	5.1@1.19	51	
Graphite	240	16.5	3.79@1.23	158.1	[84]
LCO	700	172	20.1@1.21	287.1	[103]
LFP	320	40	6.2@0.5	193.8	[111]
LCO	440	100.5	13.6@1.41	309.1	[89]
TiO2	390	10	2.3@1.68	59	[112]
Graphite	1200	50	17.25@0.93	143.8	[13]
LFP	1400	90	10.5@3.06	75	[113]
NMC811	740	155	29@1.47	391.9	[40]
2 μm Si	210	15	45@1.79	2142	
LFP	800	60	5.7@1	71.3	[52]
NCA	600	73.8	13@1.48	216.7	[97]
NMC622	161	46	8.1@0.83	503.1	[114]
LTO	600	168	26.5@1.68	441.7	[57]
S	300	6	6.9@1	230	[99]
LFP	1000	128	19.6@1	196	[9]
NMC622	220	61.38	10.93@1.1	496.8	[115]
NMC622	154	37.6	6.58@0.38	427.3	[2]
Graphite	182	23.4	7.84@0.82	430.8	
NMC532	240	30	5.84@1.15	228.3	[28]
NMC622	250	51.7	8.79@0.93	351.6	[92]
NMC111	1710	320	45.4@4.96	265.5	[116]
NMC111	320	72	9.86@1.12	308.3	[31]
Graphite	320	43	11.23@1.62	352.1	
NMC111	322	60	5.1@1.8	158.4	[47]
LFP	1350	108	15.9@3.6	117.8	[117]
LTO	550	110	11.11@1.6	202	[68]
LFP	500	90	11.07@1.23	221.4	
LFP	430	46.5	7.2@1	167.4	[56]
LCO	1500	206	24.5@1.44	163.8	[88]

This chapter gives the recent efforts on improving the CCT and the LPD to construct thicker electrodes. It must emphasize again that the first law of thick electrodes is to obtain high performance electrodes with high mass loading and high accessible areal capacity, not for larger thickness. Some thick electrodes constructed by the above methods show lower volumetric specific capacity that have no competition with the traditional

 doi:10.20944/preprints202212.0437.v1

electrodes. And some design of thick electrodes cannot be transferred directly to state-of-the-art large scale cell manufacturing processes in industry. Table 1 gives the summary of the thick electrodes. And the volumetric specific capacity of thick electrodes is not below 400 mAh·cm^{-3} which is the current level of traditional electrodes.

4. Conclusion and outlook

Recently moving towards carbon neutrality has become a global consensus and the green transportation attracts more attention. The EVs with the driving range of above 500 km could get more competitive to survive in the market for automobiles. And a practicable way to reach this value is to adopt thick electrodes with high mass loading and high area capacity. The obstacles stand in the way of using thick electrodes are weak mechanical stability and poor electrochemical performance, or are limited by the CCT and the LPD. Here, the understanding of these mechanisms and the recent efforts on breaking the limitations are given.

The design of thick electrodes is aimed at obtaining higher energy density of LIBs at battery pack level, and the thickness is just an appearance. The larger thickness does not necessarily imply more benefits. With the trade-off between energy and cost, the larger thickness has negligible impacts on improving energy density of LIBs at battery pack level and has negative effects on the cost of LIBs. In addition, some thick electrodes with low volumetric capacity go against the original intention of this design. A specific capacity of not below 400 mAh·cm-3 is needed for long-range EVs.

The design of thick electrodes is aimed at applications for practical use like EVs, and the preparation process must be suitable for a large-scale use. Some methods for fabricating thick electrodes are only for a laboratory scale. Some technologies with drying process may cause the microstructural heterogeneity in the electrodes due to the drying-induced migration of the binder to the electrode surface. And combining with the requirement of low-cost solution, some solvent-free manufacturing technologies are appropriate like dry-coated technique which is suitable for the mass manufacture and cuts cost of using and removing the toxic solvents. And an environment friendly industry is more easily be accepted by local government and residents.

The electrochemical performance is the most basic requirements for thick electrodes. Decreasing the tortuosity of thick electrodes by fabricating ordered microchannels paralleling the diffusion of Li+ has been considered as the most effective ways to help thick electrodes in performing better properties. Due to the low-tortuosity design resulted to active mass loss, it is essential to precisely construct vertical channels. From the studies on constructing aligned pathways, the laser-ablation process could be better controlled to precisely adjust parameters of the vertical channels.

Funding: The work is supported by China Shenhua Coal to Liquid and Chemical Shanghai Research Institute, Grant No. SAC-B-CT-TECH-2022-04-25, and National Science Foundation of China, Grant No. 51777140, and the Fundamental Research Funds for the Central Universities at Tongji University, Grant No. 17002150019.

Conflicts of Interest: The funders had no role in the design of the study; in the collection, analyses, or interpretation of data; in the writing of the manuscript; or in the decision to publish the results.

References

1. High energy high power battery exceeding PHEV-40 requirements. https://www.energy.gov/sites/prod/files/2015/06/f23/es209_rempel_2015_p.pdf.
2. K. G. Gallagher; S. E. Trask. Optimizing Areal Capacities through Understanding the Limitations of Lithium-Ion Electrodes. *J. Electrochem. Soc.* **2015,** *163* (2), A138-A149.
3. O. Gröger; H. A. Gasteiger. Review—Electromobility: Batteries or Fuel Cells? *J. Electrochem. Soc.* **2015,** *162* (14), A2605-A2622.
4. D. Andre; S.-J. Kim. Future generations of cathode materials: an automotive industry perspective. *Journal of Materials Chemistry A* **2015,** *3* (13), 6709-6732.
5. Technology roadmap of clean and new energy vehicles 2.0. http://zhishi.sae-china.org/ppt.html?id=2100.

6. C. Xia; C. Kwok. A high-energy-density lithium-oxygen battery based on a reversible four-electron conversion to lithium oxid. *Science* **2018,** *361* (6404), 777-781.
7. J. Zhang; P. F. Wang. Interfacial Design for a 4.6 V High-Voltage Single-Crystalline LiCoO2 Cathode. *Adv. Mater.* **2022,** *34* (8), e2108353.
8. K. Du; R. Tao. In-situ synthesis of porous metal fluoride@carbon composite via simultaneous etching/fluorination enabled superior Li storage performance. *Nano Energy* **2022,** *103*.
9. B. Shi; Y. Shang. Low Tortuous, Highly Conductive, and High-Areal-Capacity Battery Electrodes Enabled by Through-thickness Aligned Carbon Fiber Framework. *Nano Lett.* **2020,** *20* (7), 5504-5512.
10. W. Pfleging A review of laser electrode processing for development and manufacturing of lithium-ion batteries. *Nanophotonics* **2018,** *7* (3), 549-573.
11. J. Liu; Z. Bao. Pathways for practical high-energy long-cycling lithium metal batteries. *Nature Energy* **2019,** *4* (3), 180-186.
12. H. Zheng; J. Li. A comprehensive understanding of electrode thickness effects on the electrochemical performances of Li-ion battery cathodes. *Electrochim. Acta* **2012,** *71*, 258-265.
13. J. S. Wang; P. Liu. Formulation and characterization of ultra-thick electrodes for high energy lithium-ion batteries employing tailored metal foams. *J. Power Sources* **2011,** *196* (20), 8714-8718.
14. K. Singh; M. Tirumkudulu Cracking in drying colloidal films. *Phys. Rev. Lett.* **2007,** *98* (21), 218302.
15. R. Chiu; T. Garino. Drying of Granular Ceramic Films: I, Effect of Processing Variables on Cracking Behavior. *J. Am. Ceram. Soc.* **1993,** *76* (9), 2257-2264.
16. V. Slowik; J. Ju Discrete modeling of plastic cement paste subjected to drying. *Cem. Concr. Compos.* **2011,** *33* (9), 925-935.
17. M. Tirumkudulu; W. Russel Cracking in drying latex films. *Langmuir* **2005,** *21* (11), 4938-4948.
18. S. Tambio; F. Cadiou. The Concept of Effective Porosity in the Discharge Rate Performance of High-Density Positive Electrodes for Automotive Application. *J. Electrochem. Soc.* **2020,** *167* (16).
19. C. Lu; Q. Huang. High-performance silicon nanocomposite based ionic actuators. *Journal of Materials Chemistry A* **2020,** *8* (18), 9228-9238.
20. L. Yan; L. Yudong. Research on the Penetration Depth in Aluminum Reduction Cell with New Type of Anode and Cathode Structures. *JOM* **2014,** *66* (7), 1202-1209.
21. R. Fang; S. Zhao. 3D Interconnected Electrode Materials with Ultrahigh Areal Sulfur Loading for Li-S Batteries. *Adv. Mater.* **2016,** *28* (17), 3374-3382.
22. G. Li; T. Ouyang. All-carbon-frameworks enabled thick electrode with exceptional high-areal-capacity for Li-Ion storage. *Carbon* **2021,** *174*, 1-9.
23. R. Woodward; F. Markoulidis. Carbon foams from emulsion-templated reduced graphene oxide polymer composites: electrodes for supercapacitor devices. *Journal of Materials Chemistry A* **2018,** *6* (4), 1840-1849.
24. H. Sun; L. Mei. Three-dimensional holey-graphene/niobia composite architectures for ultrahigh-rate energy storage. *Science* **2017,** *356* (6338), 599-604.
25. J. Kang; H. Q. Pham. Improved rate capability of highly loaded carbon fiber-interwoven LiNi 0.6 Co 0.2 Mn 0.2 O 2 cathode material for high-power Li-ion batteries. *J. Alloys Compd.* **2016,** *657*, 464-471.
26. F. Shen; W. Luo. Ultra-Thick, Low-Tortuosity, and Mesoporous Wood Carbon Anode for High-Performance Sodium-Ion Batteries. *Advanced Energy Materials* **2016,** *6* (14).
27. M. Ebner; D.-W. Chung. Tortuosity Anisotropy in Lithium-Ion Battery Electrodes. *Advanced Energy Materials* **2014,** *4* (5).
28. R. Xiong; Y. Zhang. Scalable Manufacture of High‐Performance Battery Electrodes Enabled by a Template‐Free Method. *Small Methods* **2021,** *5* (6).
29. L. Zhang; Y. Pan. Designing vertical channels with expanded interlayers for Li-ion batteries. *Chem. Commun.* **2019,** *55* (29), 4258-4261.
30. Y. Xia; T. S. Mathis. Thickness-independent capacitance of vertically aligned liquid-crystalline MXenes. *Nature* **2018,** *557* (7705), 409-412.
31. M. Singh; J. Kaiser. Thick Electrodes for High Energy Lithium Ion Batteries. *J. Electrochem. Soc.* **2015,** *162* (7), A1196-A1201.
32. Y. Kato; S. Shiotani. All-Solid-State Batteries with Thick Electrode Configurations. *The Journal of PhysIcal Chemistry Letters* **2018,** *9* (3), 607-613.
33. A. Kubanska; L. Castro. Effect of composite electrode thickness on the electrochemical performances of all-solid-state li-ion batteries. *J. Electroceram.* **2017,** *38* (2-4), 189-196.
34. S.-B. Hong; Y.-J. Lee. All-Solid-State Lithium Batteries: Li+-Conducting Ionomer Binder for Dry-Processed Composite Cathodes. *ACS Energy Letters* **2022,** *7* (3), 1092-1100.
35. H. Cheng; K. Li Charge delivery goes the distance. *Science* **2017,** *356* (6338), 582-583.
36. Y. Kuang; C. Chen. Thick Electrode Batteries: Principles, Opportunities, and Challenges. *Advanced Energy Materials* **2019,** *9* (33).
37. A. Kukay; R. Sahore. Aqueous Ni-rich-cathode dispersions processed with phosphoric acid for lithium-ion batteries with ultra-thick electrodes. *J. Colloid Interface Sci.* **2021,** *581* (Pt B), 635-643.
38. H. Li Practical Evaluation of Li-Ion Batteries. *Joule* **2019,** *3* (4), 911-914.
39. Z. Du; K. M. Rollag. Enabling aqueous processing for crack-free thick electrodes. *J. Power Sources* **2017,** *354*, 200-206.
40. S.-H. Park; P. J. King. High areal capacity battery electrodes enabled by segregated nanotube networks. *Nature Energy* **2019,** *4* (7), 560-567.

41. H. Gao; Q. Wu. Revealing the Rate-Limiting Li-Ion Diffusion Pathway in Ultrathick Electrodes for Li-Ion Batteries. *The Journal of Physical Chemistry Letters* **2018,** *9* (17), 5100-5104.
42. Z. Li; L. Yin. Synchrotron Operando Depth Profiling Studies of State-of-Charge Gradients in Thick Li(Ni0.8Mn0.1Co0.1)O2 Cathode Films. *Chem. Mater.* **2020,** *32* (15), 6358-6364.
43. H. Shin; J. Santamarina Desiccation cracks in saturated fine-grained soils: particle-level phenomena and effective-stress analysis. *Géotechnique* **2011,** *61* (11), 961-972.
44. P. Lura; B. Pease. Influence of Shrinkage-Reducing Admixtures on Development of Plastic Shrinkage Cracks. *ACI Mater. J.* **2007,** *104* (2), 187-194.
45. E. R. Dufresne; E. I. Corwin. Flow and fracture in drying nanoparticle suspensions. *Phys. Rev. Lett.* **2003,** *91* (22), 224501.
46. N. Birk-Braun; K. Yunus. Generation of strength in a drying film: How fracture toughness depends on dispersion properties. *Phys. Rev. Lett.* **2017,** *95* (2-1), 022610.
47. L. Ibing; T. Gallasch. Towards water based ultra-thick Li ion battery electrodes – A binder approach. *J. Power Sources* **2019,** *423*, 183-191.
48. J. Kumberg; M. Müller. Drying of Lithium - Ion Battery Anodes for Use in High - Energy Cells: Influence of Electrode Thickness on Drying Time, Adhesion, and Crack Formation. *Energy Technology* **2019,** *7* (11).
49. J. Hu; B. Wu. Evolution of the rate-limiting step: From thin film to thick Ni-rich cathodes. *J. Power Sources* **2020,** *454*.
50. W.Appiah; J. Park. Design optimization of $LiNi_{0.6}Co_{0.2}Mn_{0.2}O_2$/graphite lithium-ion cells based on simulation and experimental data. *J. Power Sources* **2016,** *319*, 147-158.
51. C. Xu; Q. Li. Femtosecond laser drilled micro-hole arrays in thick and dense 2D nanomaterial electrodes toward high volumetric capacity and rate performance. *J. Power Sources* **2021,** *492*.
52. C. Chen; Y. Zhang. Highly Conductive, Lightweight, Low - Tortuosity Carbon Frameworks as Ultrathick 3D Current Collectors. *Advanced Energy Materials* **2017,** *7* (17).
53. R. Sahore; D. L. Wood. Towards Understanding of Cracking during Drying of Thick Aqueous-Processed LiNi0.8Mn0.1Co0.1O2 Cathodes. *ACS Sustainable Chemistry & Engineering* **2020,** *8* (8), 3162-3169.
54. G. F. Yang; K. Y. Song. A metal foam as a current collector for high power and high capacity lithium iron phosphate batteries. *Journal of Materials Chemistry A* **2014,** *2* (46), 19648-19652.
55. Z. Yang; J. Tian. High energy and high power density supercapacitor with 3D Al foam-based thick graphene electrode: Fabrication and simulation. *Energy Storage Materials* **2020,** *33*, 18-25.
56. G.-F. Yang; K.-Y. Song. Ultra-thick Li-ion battery electrodes using different cell size of metal foam current collectors. *RSC Advances* **2015,** *5* (22), 16702-16706.
57. L. Hu; F. La Mantia. Lithium-Ion Textile Batteries with Large Areal Mass Loading. *Advanced Energy Materials* **2011,** *1* (6), 1012-1017.
58. M. Al-Shroofy; Q. Zhang. Solvent-free dry powder coating process for low-cost manufacturing of LiNi1/3Mn1/3Co1/3O2 cathodes in lithium-ion batteries. *J. Power Sources* **2017,** *352*, 187-193.
59. D.-W. Park; N. A. Cañas. Novel solvent-free direct coating process for battery electrodes and their electrochemical performance. *J. Power Sources* **2016,** *306*, 758-763.
60. X. Qin; X. Wang. Hierarchically porous and conductive LiFePO4 bulk electrode: binder-free and ultrahigh volumetric capacity Li-ion cathode. *J. Mater. Chem.* **2011,** *21* (33).
61. R. Elango; A. Demortière. Thick Binder - Free Electrodes for Li–Ion Battery Fabricated Using Templating Approach and Spark Plasma Sintering Reveals High Areal Capacity. *Advanced Energy Materials* **2018,** *8* (15).
62. C. Sun; S. Liu. 3D printing nanocomposite gel-based thick electrode enabling both high areal capacity and rate performance for lithium-ion battery. *Chem. Eng. J.* **2020,** *381*.
63. X. Tang; H. Zhou. Generalized 3D Printing of Graphene-Based Mixed-Dimensional Hybrid Aerogels. *ACS Nano* **2018,** *12* (4), 3502-3511.
64. X. Gao; X. Yang. Converting a thick electrode into vertically aligned "Thin electrodes" by 3D-Printing for designing thickness independent Li-S cathode. *Energy Storage Materials* **2020,** *24*, 682-688.
65. S. M. Sajadi; S. Enayat. Three-dimensional printing of complex graphite structures. *Carbon* **2021,** *181*, 260-269.
66. M. Sotomayor; C. Torre-Gamarra. Additive-free $Li_4Ti_5O_{12}$ thick electrodes for Li-ion batteries with high electrochemical performance. *Journal of Materials Chemistry A* **2018,** *6* (14), 5952-5961.
67. C. de la Torre-Gamarra; M. E. Sotomayor. High mass loading additive-free LiFePO4 cathodes with 500 μm thickness for high areal capacity Li-ion batteries. *J. Power Sources* **2020,** *458*.
68. M. E. Sotomayor; C. d. l. Torre-Gamarra. Ultra-thick battery electrodes for high gravimetric and volumetric energy density Li-ion batteries. *J. Power Sources* **2019,** *437*.
69. H. Duong; J. Shin. *Dry Electrode Coating Technology*; Maxwell Technologies, Inc.
70. B. Ludwig; Z. Zheng. Solvent-Free Manufacturing of Electrodes for Lithium-ion Batteries. *Scientific Reports* **2016,** *6*, 23150.
71. K. Fu; Y. Yao. Progress in 3D Printing of Carbon Materials for Energy-Related Applications. *Adv. Mater.* **2017,** *29* (9).
72. Y. Yoon; K. Lee. Vertical alignments of graphene sheets spatially and densely piled for fast ion diffusion in compact supercapacitors. *ACS Nano* **2014,** *8* (5), 4580-90.
73. P. A. Johns; M. R. Roberts. How the electrolyte limits fast discharge in nanostructured batteries and supercapacitors. *Electrochem. Commun.* **2009,** *11* (11), 2089-2092.

74. N. Ogihara; Y. Itou. Impedance Spectroscopy Characterization of Porous Electrodes under Different Electrode Thickness Using a Symmetric Cell for High-Performance Lithium-Ion Batteries. *The Journal of Physical Chemistry C* **2015,** *119* (9), 4612-4619.
75. B.BVijayaraghavan; D. Ely. An Analytical Method to Determine Tortuosity in Rechargeable Battery Electrodes. *J. Electrochem. Soc.* **2012,** *159* (5), A548-A552.
76. S. Harris; P. Lu Effects of Inhomogeneities—Nanoscale to Mesoscale—on the Durability of Li-Ion Batteries. *The Journal of Physical Chemistry C* **2013,** *117* (13), 6481-6492.
77. M. Ebner; V. Wood Tool for Tortuosity Estimation in Lithium Ion Battery Porous Electrodes. *J. Electrochem. Soc.* **2015,** *162* (2), A3064-A3070.
78. H. Li; Y. Tao. Ultra-thick graphene bulk supercapacitor electrodes for compact energy storage. *Energy & Environmental Science* **2016,** *9* (10), 3135-3142.
79. Q. Xiao; M. Gu. Inward lithium-ion breathing of hierarchically porous silicon anodes. *Nature Communication* **2015,** *6*, 8844.
80. V. Ramadesigan; R. N. Methekar. Optimal Porosity Distribution for Minimized Ohmic Drop across a Porous Electrode. *J. Electrochem. Soc.* **2010,** *157* (12).
81. S. Golmon; K. Maute. Multiscale design optimization of lithium ion batteries using adjoint sensitivity analysis. *International Journal for Numerical Methods in Engineering* **2012,** *92* (5), 475-494.
82. S. Golmon; K. Maute. A design optimization methodology for Li^+ batteries. *J. Power Sources* **2014,** *253*, 239-250.
83. Y. Qi; T. Jang. Is There a Benefit in Employing Graded Electrodes for Lithium-Ion Batteries? *J. Electrochem. Soc.* **2017,** *164* (13), A3196-A3207.
84. B. Bitsch; T. Gallasch. Capillary suspensions as beneficial formulation concept for high energy density Li-ion battery electrodes. *J. Power Sources* **2016,** *328*, 114-123.
85. C. P. Wang; S. D. Lopatin. Graded electrode technologies for high energy lithium-ion batteries. 20110168550, 2011.
86. C. Huang; M. Dontigny. Low-tortuosity and graded lithium ion battery cathodes by ice templating. *Journal of Materials Chemistry A* **2019,** *7* (37), 21421-21431.
87. V. Kolosnitsyn; E. Karaseva Improvements relating to electrode structures in batteries. 2006010894, 2006.
88. L. L. Lu; Y. Y. Lu. Wood-Inspired High-Performance Ultrathick Bulk Battery Electrodes. *Adv. Mater.* **2018,** *30* (20), e1706745.
89. L. Li; R. M. Erb. Fabrication of Low - Tortuosity Ultrahigh - Area - Capacity Battery Electrodes through Magnetic Alignment of Emulsion - Based Slurries. *Advanced Energy Materials* **2018,** *9* (2).
90. J. S. Sander; R. M. Erb. High-performance battery electrodes via magnetic templating. *Nature Energy* **2016,** *1* (8).
91. J. Park; S. Hyeon. Performance enhancement of Li-ion battery by laser structuring of thick electrode with low porosity. *Journal of Industrial and Engineering Chemistry* **2019,** *70*, 178-185.
92. P. Zhu; H. J. Seifert. The Ultrafast Laser Ablation of Li(Ni0.6Mn0.2Co0.2)O2 Electrodes with High Mass Loading. *Applied Sciences* **2019,** *9* (19).
93. N. Huebsch; D. J. Mooney Inspiration and application in the evolution of biomaterials. *Nature* **2009,** *462* (7272), 426-32.
94. Y. Ma; D. Yao. Ultra-thick wood biochar monoliths with hierarchically porous structure from cotton rose for electrochemical capacitor electrodes. *Electrochim. Acta* **2020,** *352*.
95. K. Liu; R. Mo. Nature-derived, structure and function integrated ultra-thick carbon electrode for high-performance supercapacitors. *Journal of Materials Chemistry A* **2020,** *8* (38), 20072-20081.
96. Z. Lv; M. Yue. Controllable Design Coupled with Finite Element Analysis of Low - Tortuosity Electrode Architecture for Advanced Sodium - Ion Batteries with Ultra - High Mass Loading. *Advanced Energy Materials* **2021,** *11* (17).
97. S. Behr, Amin, R., Chiang, Y. M. & Tomsia, A. P. Highly structured, additive free lithium-ion cathodes by freeze-casting technology. *Ceram. Forum Int.* **2015,** *92*, E39-E43.
98. J. Billaud; F. Bouville. Magnetically aligned graphite electrodes for high-rate performance Li-ion batteries. *Nature Energy* **2016,** *1* (8).
99. J. Ma; Y. Qiao. Low tortuosity thick cathode design in high loading lithium sulfur batteries enabled by magnetic hollow carbon fibers. *Appl. Surf. Sci.* **2021,** *542*.
100. G. Pan; L. Hu. Out-of-Plane Alignment of Conjugated Semiconducting Polymers by Horizontal Rotation in a High Magnetic Field. *The Journal of PhysIcal Chemistry Letters* **2021,** *12* (14), 3476-3484.
101. X. Li; H. Zhao. High - Efficiency Alignment of 3D Biotemplated Helices via Rotating Magnetic Field for Terahertz Chiral Metamaterials. *Advanced Optical Materials* **2019,** *7* (12).
102. K.-H. Chen; M. J. Namkoong. Efficient fast-charging of lithium-ion batteries enabled by laser-patterned three-dimensional graphite anode architectures. *J. Power Sources* **2020,** *471*.
103. J. Park; C. Jeon. Challenges, laser processing and electrochemical characteristics on application of ultra-thick electrode for high-energy lithium-ion battery. *J. Power Sources* **2021,** *482*.
104. M. Mangang; H. J. Seifert. Influence of laser pulse duration on the electrochemical performance of laser structured LiFePO4 composite electrodes. *J. Power Sources* **2016,** *304*, 24-32.
105. W. Pfleging; J. Pröll A new approach for rapid electrolyte wetting in tape cast electrodes for lithium-ion batteries. *Journal of Materials Chemistry A* **2014,** *2* (36), 14918-14926.
106. E. Mottay; X. Liu. Industrial applications of ultrafast laser processing. *MRS Bull.* **2016,** *41* (12), 984-992.
107. J. B. Habedank; L. Kraft. Increasing the Discharge Rate Capability of Lithium-Ion Cells with Laser-Structured Graphite Anodes: Modeling and Simulation. *J. Electrochem. Soc.* **2018,** *165* (7), A1563-A1573.

 doi:10.20944/preprints202212.0437.v1

108. M. Singh; J. Kaiser. A systematic study of thick electrodes for high energy lithium ion batteries. *J. Electroanal. Chem.* **2016,** *782*, 245-249.
109. L. Airoldi; U. Tamburini. Additive Manufacturing of Aqueous - Processed $LiMn_2O_4$ Thick Electrodes for High - Energy - Density Lithium - Ion Batteries. *Batteries & Supercaps* **2020,** *3* (10), 1040-1050.
110. J. Lee; C. Jo. Bicontinuous phase separation of lithium-ion battery electrodes for ultrahigh areal loading. *PNAS* **2020,** *117* (35), 21155-21161.
111. Y. Kuang; C. Chen. Conductive Cellulose Nanofiber Enabled Thick Electrode for Compact and Flexible Energy Storage Devices. *Advanced Energy Materials* **2018,** *8* (33).
112. U. Klotzbach; K. Washio., Femtosecond laser patterning of lithium-ion battery separator materials: impact on liquid electrolyte wetting and cell performance. In *Laser-based Micro- and Nanoprocessing IX*, 2015.
113. S.-J. Cho; K.-H. Choi. Hetero-Nanonet Rechargeable Paper Batteries: Toward Ultrahigh Energy Density and Origami Foldability. *Adv. Funct. Mater.* **2015,** *25* (38), 6029-6040.
114. L. S. Kremer; T. Danner. Influence of the Electrolyte Salt Concentration on the Rate Capability of Ultra - Thick NCM 622 Electrodes. *Batteries & Supercaps* **2020,** *3* (11), 1172-1182.
115. L. S. Kremer; A. Hoffmann. Manufacturing Process for Improved Ultra - Thick Cathodes in High - Energy Lithium - Ion Batteries. *Energy Technology* **2019,** *8* (2).
116. T. Wu; Z. Zhao. Thick electrode with thickness-independent capacity enabled by assembled two-dimensional porous nanosheets. *Energy Storage Materials* **2021,** *36*, 265-271.
117. H. Li; L. Peng. Ultrahigh-Capacity and Fire-Resistant LiFePO4
-Based Composite Cathodes for Advanced Lithium-Ion Batteries. *Advanced Energy Materials* **2019,** *9* (10).